GRASSHOPPER

Grid Assisting Modular Hydrogen PEM Power Plant

D5.6 – Report on beyond the project improvements and scale-up simulations

Authors: Elena Crespi, Giulio Guandalini, Stefano Campanari, POLIMI
Reviewers: Marijan Vidmar, INEA

Fuel Cells and Hydrogen Joint Undertaking (FCH JU)
Project 779430

March 2022

Workpackage / Task	WP 5 / T 5.2
Deliverable nature:	Report
Dissemination level:	Public
Contractual delivery date:	March 2022
Actual delivery date:	May 2022
Version:	1.0
Total number of pages:	24
Keywords:	MW-size PEM FC plant, dynamic simulations, optimization
Approved by the coordinator:	30/05/2022
Submitted to EC by the coordinator:	30/05/2022

Disclaimer

Copyright

This project has received funding from the Fuel Cells and Hydrogen 2 Joint Undertaking under grant agreement No 779430. This Joint Undertaking receives support from the European Union's Horizon 2020 research and innovation programme, Hydrogen Europe and Hydrogen Europe research.

Executive Summary

This report describes the improvements proposed for the scale-up of the GRASSHOPPER power plant to the MW-scale. The analysis includes the comparison of different layouts (including changes in components key technological features) and operation conditions though simulations, that allow assessing the plant performance. Unluckily, actual data on the prototype plant were missing at the moment of the definition of this activity, so preliminary data from FAT and other intermediate testing are used.

In details, a description of the main features of the Grasshopper pilot plant is given in Chapter 2, while the main features of the models realized to simulate the system steady state and dynamic behavior are described in Chapter 3. The steady state model, realized with the software Aspen Plus, includes a customize model of the stack, able to reproduce real cell performances through semi-empirical polarization curves, and all the Balance of Plant (BoP) components. The dynamic model, realized with the software Simulink, includes sub-models of the main plant components, mainly solving mass and energy balances during variable load operation, and PI-type and on-off controllers for the control of system operation. The dynamic model validation through comparison of simulation results and experimental data from the pilot plant FAT showed the ability of the model to reproduce the real plant performance.

Chapter 4 focuses on the presentation of the solutions to improve the layout and the operation strategy of the MW-scale system. Solutions to optimize the plant performance both at full load and at partial load are shown in Section 4.1. The adoption of multiple air compressors in parallel allows to increase the flexibility of the plant, while an increase in the stack backpressure allows increasing the plant net efficiency at high loads. The additional installation of an expander, to recover energy from the cathode exhausts, allows increasing the system net efficiency and reaching higher net power (fixed the maximum current density). Additionally, the highest net efficiency is obtained at the highest simulated backpressure for any current density, simplifying the operation strategy. Solutions to optimize the cold start-up through faster warm-up are presented in Section 4.2. Simulation results show that the warm-up time is influenced by the stack current density: higher current density allows faster warm-ups thanks to the higher thermal losses of the stack. It follows that warm-up strategies limiting the current density at low temperatures, that can be required to limit the stack degradation, may affect the plant flexibility increasing the warm-up time. Additionally, simulations results shows that the warm-up times are strongly affected by the lengths of the pipes connecting the components, highlighting the importance of designing a compact system.

Chapter 5 describes the economic evaluation with regards to the MW scale Fuel Cell Power Plant, highlighting the predominant economic items in the total MW- scale FCPP costs, and evaluates potential improvements.

Chapter 6 summarizes the main outcomes of the activity, providing recommendations for the design and operation strategies of the MW-scale system.

This project has received funding from the Fuel Cells and Hydrogen 2 Joint Undertaking under grant agreement No 779430. This Joint Undertaking receives support from the European Union's Horizon 2020 research and innovation programme, Hydrogen Europe and Hydrogen Europe research.

Document History

Version	Date	Status	Author	Comment
1.0	15/05/2022	Draft	POLIMI	complete draft

This project has received funding from the Fuel Cells and Hydrogen 2 Joint Undertaking under grant agreement No 779430. This Joint Undertaking receives support from the European Union's Horizon 2020 research and innovation programme, Hydrogen Europe and Hydrogen Europe research.

Table of Contents

This project has received funding from the Fuel Cells and Hydrogen 2 Joint Undertaking under grant agreement No 779430. This Joint Undertaking receives support from the European Union's Horizon 2020 research and innovation programme, Hydrogen Europe and Hydrogen Europe research.

1 Introduction

The GRASSHOPPER projects aims at designing a MW-size Fuel Cell (FC) power plant able to provide flexibility services to the grid. The MW-size plant is based on learning from the 100 kW sub-module pilot plant that has been finalized in September 2021, has undergone Factory Acceptance Tests (FAT) and will be demonstrated in field in Delfzij, the Netherland. While the original project plan included the plant demonstration phase, consisting in 8 months of continuous plant operation in Delfzij, delays in the plant construction have caused a postponement of this activity, that will be performed after the closure of the project.

This present works aims at giving recommendations for the design and operation strategies of the MW-scale system. Since data from plant operation in field are not available, the suggestions are based on results of the simulation activities performed within the projects. These results are however supported by the experimental data measured during the pilot plant FAT; that allowed to validate the system dynamic model through comparison of the experimental measures with the simulation results. The performed simulations include the comparison of different layouts and operation conditions, to assess the system performance and flexibility.

Since the MW-size system is based on the pilot plant layout, a description of the main features of the Grasshopper 100 kW system is given in Chapter 2. The main features of the models realized to simulate the system steady state and dynamic behavior are then described in Chapter 3. Chapter 4 focuses on the presentation of the solutions to improve the layout and the operation strategy of the MW-scale system. Solutions to optimize the plant performance both at full load and at partial load are described in Section 4.1, while solutions to optimize the cold start-up through faster warm-up are presented in Section 4.2. Chapter 5 summarizes the cost evaluation for the MW scale FCPP, and its improvements, carried out within the framework of the GRASSHOPPER project. Finally, Chapter 6 summarizes the main outcomes of the activity, providing recommendations for the design and operation strategies of the MW-scale system.

This project has received funding from the Fuel Cells and Hydrogen 2 Joint Undertaking under grant agreement No 779430. This Joint Undertaking receives support from the European Union's Horizon 2020 research and innovation programme, Hydrogen Europe and Hydrogen Europe research.

2 Pilot plant features

The Grasshopper pilot unit features an accurate design and construction, adopting improved MEAs and stack design and BoP components aiming at flexibility. The layout of the pilot plant, shown in Figure 2.1, is the result of learnings from previous experiences [1], [2] and of a preliminary simulation activity that has explored the system stationary performance at different loads, with different configuration and control strategy.

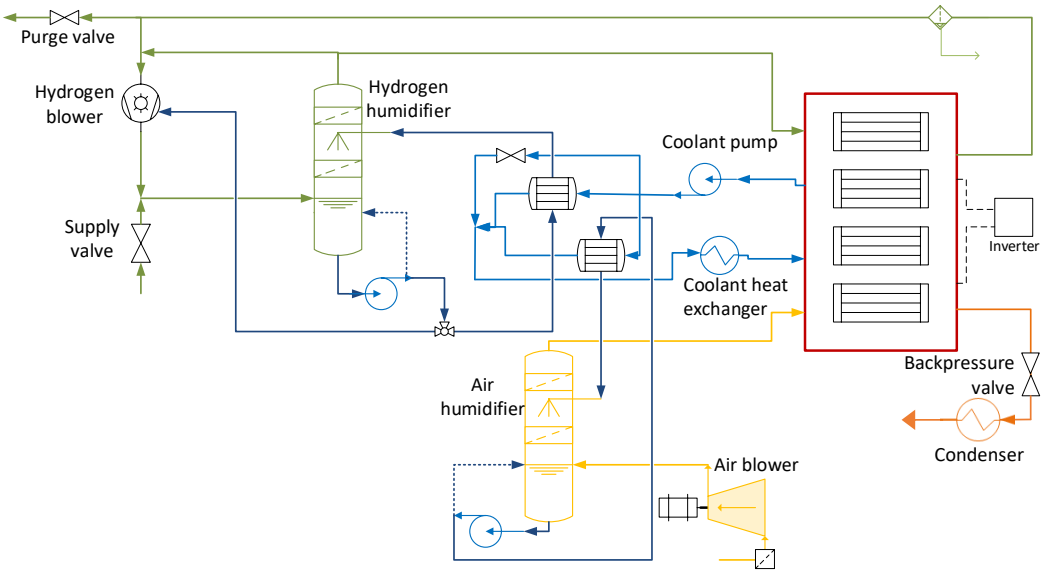

Figure 2.1 – Layout of the Grasshopper 100 kW_{el} PEM FC power plant.

The PEM FC includes several identical stacks, supplied with pure hydrogen and air. In order to enhance performance and durability of the cells, reactants humidity and pressure as well as cells temperature have to be controlled. In this respect, dedicated reactants humidifiers and a cooling circuit using water-glycol mixture have been included.

Pure hydrogen is assumed available at plant inlet at a sufficiently high pressure (above a minimum of 2 bar), avoiding a compression step. This assumption is reasonable since hydrogen comes from upstream processes or from a buffer tank that operates above atmospheric pressure. The exhaust hydrogen from the anode outlet is recirculated to increase the total hydrogen utilization factor by means of a liquid ring compressor. A purge valve on the hydrogen line avoids inert gases build-up, while fresh pure hydrogen enters the system in the humidifier.

Fresh air is compressed, humidified and fed to the FC stacks cathode. A backpressure valve is included to keep the system pressurized and operate the plant under mildly pressurized conditions. Air is then cooled to condensate the water vapor and separate the demineralized water, and finally released into the atmosphere.

Two separate circuits for air humidification and stacks cooling water are included, resulting in full controllability. The separate cooling water circuit allows to use an ethylene glycol/water mixture (50/50%vol) to cool the stacks. This option is particularly interesting for possible fully independent applications in cold climates

This project has received funding from the Fuel Cells and Hydrogen 2 Joint Undertaking under grant agreement No 779430. This Joint Undertaking receives support from the European Union's Horizon 2020 research and innovation programme, Hydrogen Europe and Hydrogen Europe research.

Both air and hydrogen humidification are performed in a shower-type packed-bed humidifier to take advantage of its scrubbing effect. A small amount of water is continuously recirculated internally to the humidifier to be filtered, while a purge removes the water produced in the FC avoiding build-up. Two heat exchangers in parallel configuration and a bypass line for control purposed allow transferring heat from the cooling circuit to both humidifiers, controlling accurately the temperature and consequently the relative humidity of the reactants at the cell inlet. Finally, the temperature of the coolant at FC stacks inlet is controlled in a dedicated heat exchanger, using a separate external cooling circuit. The coolant pump is regulated to vary the coolant flow rate maintaining the design stacks temperature at any load.

The nominal operating points and the minimum load point for the FC stack designed for the Grasshopper pilot plant, reported in Table 2.1, are also the result of learnings from previous experience and system simulations. The current density is expected to reach a minimum of 0.2 A/cm^2 during plant operation. The stack temperature setpoint remains constant for any current density, while the setpoint for the coolant temperature gain over the stack decreases proportionally to the current, reaching a minimum of 5°C at 0.2 A/cm^2. The other setpoint are independent with respect to the current density.

Table 2.1 - Stack nominal operating conditions [3] **at nominal load and at minimum load.**

	Nominal load	Minimum load
Current density	1.0 A/cm^2	0.2 A/cm^2
Air stoichiometry*	2.0	
Hydrogen stoichiometry*	1.5	
Air/Hydrogen averages RH	100 %	
Air backpressure (stack outlet)	0.1 – 0.7 bar$_g$	
Hydrogen backpressure (stack outlet)	0.1 – 0.7 bar$_g$	
Stack temperature	70 °C	
Coolant temperature gain**	10 °C	5 °C

*The terms 'air stoichiometry' ('hydrogen stoichiometry') refers to the ratio of the air (hydrogen) flow rate with respect to the stoichiometric flow rate.

**The coolant temperature gain varies linearly with the current density

In practice, the control of stack temperature, coolant temperature gain, air and hydrogen relative humidity and backpressure results very effective. On the contrary, a perfect control of the air stoichiometry result not possible only varying the rotational speed of the blower. While no problem arises at high current densities, at low current density a fraction of the compressed air has to be purged to limit the air stoichiometry. Additionally, the hydrogen flow rate processed by the liquid ring compressor is limited in a narrow range. A perfect control of the hydrogen stoichiometry is therefore not possible by regulating the liquid ring compressor speed. The possibility of recirculating the humidified hydrogen on the compressor is therefore included. These solutions allow respecting the constraints on the stack stoichiometry, but increases the compressor consumptions, negatively affecting the plant performance at partial load.

This project has received funding from the Fuel Cells and Hydrogen 2 Joint Undertaking under grant agreement No 779430. This Joint Undertaking receives support from the European Union's Horizon 2020 research and innovation programme, Hydrogen Europe and Hydrogen Europe research.

3 System models

This chapter gives an overview of the main features of the stationary and dynamic numerical models of the system that have been developed to assist the plant scale-up.

The stationary model of the flexible FC plant is set up using the process simulation tool Aspen Plus® [4], a commercial simulation code for energy and chemical plants design and rating. Models of the main plant units are found in the standard libraries of the software, with the exception of the PEM FC stacks, for which a customized model in the Aspen Custom Modeler language has been implemented. The stack model is based on a lumped-volume approach since the model aims at reproducing large scale effects. Thus, a detailed description of the internal geometry of a single cell would increase the computational cost without bringing any advantage. Additionally, since the FC model has a modular structure, the lumped model is realized for a single cell. Several identical cells are then electrically connected in series to build a stack and the stacks are in turn electrically connected in parallel and/or in series to reach the desired FC size. The 0D model is able to calculate the produced power on the base of regressed semi-empirical polarization curves and to solve mass and energy balances on the stacks to determine outlet gas flows composition and temperature. The properties of the BoP component models are obtained from the datasheet of the components installed in the pilot plant. Additional detail on the stationary model of the system are reported in Deliverable 5.2 and Deliverable D5.3 and have been published in [5].

The dynamic model of the system is realized with the software Simulink, and includes sub-models of the main plant components, mainly solving mass and energy balances during variable load operation. As in the stationary model, the stack electrochemical performance are calculated through semi-empirical current-voltage polarization curves. Fluid properties are calculated for the gas with the hypothesis of ideal gas and ideal gas mixture, and for the liquid considering ideal liquid with constant specific heat. The single component models are then combined into the plant model and PI-type and on/off type controllers are implemented for the control of the system operation. A first model has been developed to simulate the 100 kW pilot plant and its ability to reproduce the real plant behavior has been validated through comparison of simulation results and experimental data from the FAT. The comparison has shown that the numerical model reproduces with a good accuracy both the behavior of the components at different load conditions (e.g. stationary values of pressure, temperature, power consumptions, etc.) and the system dynamics (e.g. thermal transients, effects related to delays in mass transfer, etc.). The validated model has been scaled-up to assess the performance of a 1 MW system, adopting the same layout configuration of the 100 kW plant. Additional details on the dynamic model of the system can be found in Deliverable D5.4 and Deliverable D5.5.

This project has received funding from the Fuel Cells and Hydrogen 2 Joint Undertaking under grant agreement No 779430. This Joint Undertaking receives support from the European Union's Horizon 2020 research and innovation programme, Hydrogen Europe and Hydrogen Europe research.

4 Proposed improvements in MW-scale plant layout and operation

This chapter collects the results of system simulations performed to find out how to improve the design of the MW-scale plant. Simulations include plant operation with different control strategies but also changes in the plant layout and components. All simulations refer to a 1 MW unit, defined by the project consortium as the size of the basic module that can be replicated to build bigger systems.

Section 4.1 describes the application of the stationary model of the system to optimize the layout and the operating point of the MW-size system. Results of this simulation activity have been published in [5].

Section 4.2 describes the application of the dynamic model of the MW-size unit to assess the flexibility of a system reflecting the layout of the 100 KW unit. The simulations focuse on the system start-up, identifying the main criticalities and proposing solutions to speed-up the warm-up phase.

4.1 Steady-state partial-load performance optimization

The stationary model has been applied to define the optimal design and operating point of the 1 MW PEM FC unit. The simulations include the comparison of different plant layouts. In details, Section 4.1.1 compares different solutions for air compression, assessing the use of multiple compression units properly arranged to meet the plant flexibility target (i.e., to grant the appropriate operating conditions in the full load range of the FC). Then, Section 4.1.2 considers the installation of air expander units, to recover energy from the FC cathode exhaust air in order to drive the air compressors.

For each case, the plant performances are analyzed for currents ranging from 20% to 150% of the nominal value (0.2 to 1.5 A/cm^2), since the plant has to work at variable load to provide ancillary services to the electric grid. Additionally, different operating conditions for the FC stack are analyzed. In particular, the results here reported considers different pressure levels (from ambient pressure to mildly pressurized conditions, up to 0.7 bar$_g$), since backpressure variations lead to the most interesting results.

The performance indexes used to assess the plant performances are gross efficiency and net efficiency. The gross efficiency, defined in equation (4.1), considers the PEM fuel cell only. The net efficiency, defined in equation (4.2), represents the overall efficiency of the plants: electrical production is depurated from the DC/AC inverter losses and from auxiliary power consumptions, including compressors and pumps consumptions, and expander generation (when present). The energy input to the system is computed according to the Lower Heating Value (LHV) of the consumed hydrogen.

$$\eta_{GROSS} = \frac{P_{FC}}{\dot{m}_{H_2} \cdot LHV} \quad \textbf{(4.1)}$$

$$\eta_{NET} = \frac{P_{FC} \cdot \eta_{inverter} - P_{auxiliaries}}{\dot{m}_{H_2} \cdot LHV} = \frac{P_{NET}}{\dot{m}_{H_2} \cdot LHV} \quad \textbf{(4.2)}$$

This project has received funding from the Fuel Cells and Hydrogen 2 Joint Undertaking under grant agreement No 779430. This Joint Undertaking receives support from the European Union's Horizon 2020 research and innovation programme, Hydrogen Europe and Hydrogen Europe research.

The stack performance depends only on the stack operating conditions, that are equal to the nominal values in all the simulations. The gross power output and the corresponding gross efficiency, obtained with current density ranging from 0.2 to 1.5 A/cm^2, are shown in Figure 4.1. For any given gross power output, the gross efficiency increases by rising the backpressure and the highest gross efficiency is obtained with the highest simulated value of backpressure (0.7 bar$_g$). Therefore, by pressurizing the cells it is possible to obtain the same gross power with a lower current density and higher cell efficiency. At the same time, since the range of currents in which the cells operate is fixed (20%-150% of nominal current), with higher backpressure it is possible to generate slightly higher gross power. The maximum generated gross power increases from 1343 kW to nearly 1441 kW moving from 0.1 bar$_g$ to 0.7 bar$_g$. Therefore, from the point of view of the fuel cell alone, pressurization appears to be always favorable.

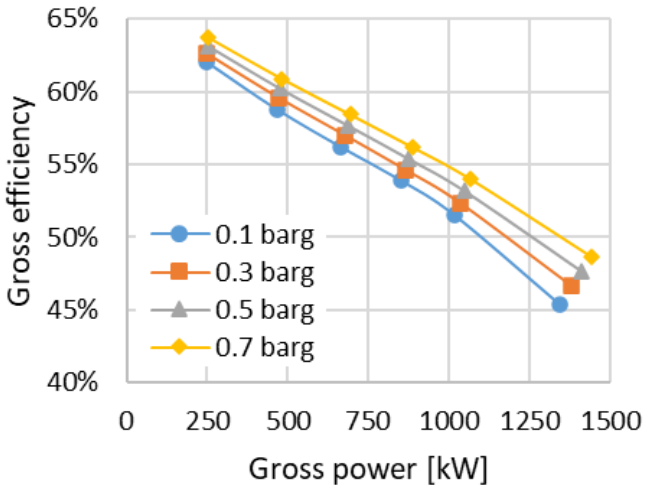

Figure 4.1 - Gross efficiency Vs Gross power, for current densities ranging between 20% and 150% of the nominal value and for different levels of stack pressurization.

4.1.1 Use of multiple air blowers in parallel configuration

The pilot plant adopts a volumetric blower to supply the stack with air. The preliminary plant tests and the 100 kW plant simulations have shown that the unit does not allow a perfect control of the air stoichiometry to the stack over the entire plant current range. Indeed, the minimum load of the blower provides an air flowrate much higher than the one required at the stack minimum load (20% of the nominal current density). A fraction of the compressed air is therefore purged, negatively affecting the plant net efficiency.

This section aims at improving the plant flexibility of the 1 MW system, optimizing the net efficiency at partial load. Considering the required pressure increase and the nominal flow rates, air compression is based on the use of volumetric blowers, as in the 100 kW plant. Three models of rotary lobe compressors are selected, able to treat different air flow rates, as detailed in Table 4.1. Based on contacts with manufacturers, it is assumed that the variable frequency-controlled motor allows, by changing the blower rotational speed, to decrease the air flow rate down to 15% of the maximum value. Calculation of the component performance is based on the blowers' efficiency curves.

This project has received funding from the Fuel Cells and Hydrogen 2 Joint Undertaking under grant agreement No 779430. This Joint Undertaking receives support from the European Union's Horizon 2020 research and innovation programme, Hydrogen Europe and Hydrogen Europe research.

Table 4.1 - Blowers main features [6].

Compressor type	Max flow rate [m^3/h]	Engine power [kW]
COMP-A	9120	355
COMP-B	5480	200
COMP-C	3540	132

Considering the range of air flow rates required by the plant at different loads (from 0.2 to 1.5 A/cm^2) and air ratios to stoichiometry (from 2 to 3), three different compression solutions are compared in order to find the configuration that allows to supply air to the FC stacks while minimizing the power consumptions:

1) one compressor COMP-A, able to process the maximum air flow required by the fuel cell;
2) two compressors COMP-B, in parallel configuration;
3) three compressors COMP-C, in parallel configuration.

A minimum and maximum pressure gain equal to 0.2 and 0.8 bar, respectively, are considered. For these extreme cases, Figure 4.2 shows the rotational speed of each analyzed compression solution as a function of the air flowrate. It results that, one compressor COMP-A makes possible the operation at maximum load and maximum air stoichiometry at any considered pressure. On the contrary, at low pressure and below ~0.48 A/cm^2 it is not possible to have air stoichiometry equal to 2; while below ~0.35 A/cm^2 the air stoichiometry cannot be lower than 3. Thus, bleeding of a fraction of air after compression would be required in order to control the air stoichiometry, limiting the plant efficiency. A single COMP-B compressor allows an air stoichiometry equal to 3 at low pressure and minimum load (0.2 A/cm^2). A maximum air flow of 1.8 kg/s is provided at high pressure, that is not sufficient to work at maximum load (1.5 A/cm^2), neither with air stoichiometry equal to 2 nor 3. Hence, the installation of a second compressor COMP-B in parallel configuration is needed. With one compressor COMP-C it is possible to work at the minimum load and air stoichiometry equal to 2, without any air bleeding. However, two compressors of this type in parallel configuration are necessary to increase the current above ~1.1 A/cm^2 while keeping the air stoichiometry at 2, and three compressors are required for the plant to work at maximum load and air stoichiometry equal to 3. Additionally, it can be observed that the operating ranges of parallel units are overlapping, allowing in certain air flow ranges to operate the system with a different number of active machines (e.g. a single unit at high load or two units at low rotational speed) and frequent start-up or shutdown of the units can be avoided.

Comparing the electrical power consumptions, no substantial differences are found by varying the compression solutions. The choice of the compressor should be driven by the possibility of a more accurate control of the plant and by economic reasons.

This project has received funding from the Fuel Cells and Hydrogen 2 Joint Undertaking under grant agreement No 779430. This Joint Undertaking receives support from the European Union's Horizon 2020 research and innovation programme, Hydrogen Europe and Hydrogen Europe research.

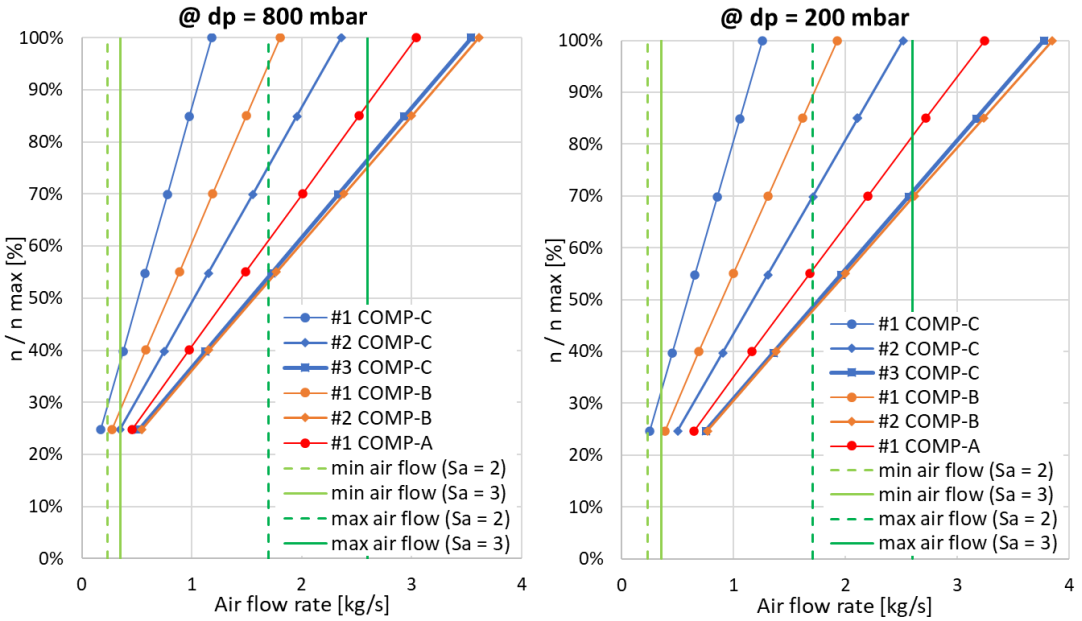

Figure 4.2 - Air compressor rotational speed as a function of the air flow rate and compressor choice, with pressure gain 800 mbar (left side) and 200 mbar (right side).

Simulations in the following are carried out considering the intermediate solution, which represents a reasonable compromise: the installation of two compressors COMP-B in parallel. It is assumed that only one compressor is activated at low current density and that the second compressor is switched on when the first one reaches the 80% of its maximum rotational speed, that is for an air flow rate of about 1.4 kg/s.

To study the effects of pressurization of the net efficiency, the consumptions of the auxiliaries (i.e., pumps and compressors) are analyzed for different pressures.

The share of gross power that is consumed by the auxiliaries is shown in Figure 4.3 for operation at nominal current, with minimum and maximum backpressure. The share of power consumption related to the compressors results always above 87% of the total auxiliary consumption. Similar results are obtained for different currents and at intermediate pressures.

The compressors power consumption is shown as a function of the gross power in Figure 4.4. As expected, the air compressors consumption increases by increasing the FC gross power (due to the increased air flow processed) and by increasing the FC stacks backpressure (due to the increased pressure change). On the contrary, the hydrogen compressor works with a narrow range of volumetric flow rates, therefore its consumption variation is mainly determined by the variation in the pressure gain that it has to provide. This last parameter depends on the pressure drop in the hydrogen recirculation loop that is proportional to the volumetric flow rate. Therefore, the hydrogen compressor consumption increases by increasing the FC gross power (higher current density, hence higher hydrogen flow to the FC stacks) but decreases by increasing the FC stack backpressure (lower volumetric flow rate at higher pressures, for a given mass flow rate).

This project has received funding from the Fuel Cells and Hydrogen 2 Joint Undertaking under grant agreement No 779430. This Joint Undertaking receives support from the European Union's Horizon 2020 research and innovation programme, Hydrogen Europe and Hydrogen Europe research.

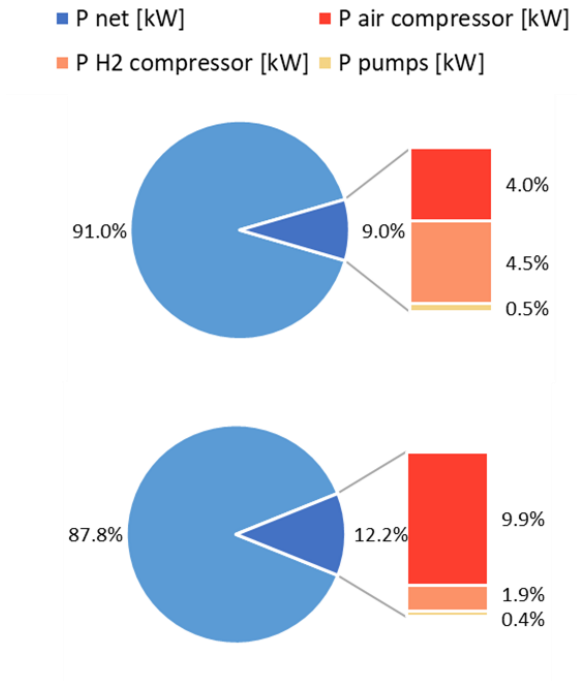

Figure 4.3 – Share of auxiliary consumption on the gross power production, at nominal current density (i = 1 A/cm^2) with cathode backpressure equal to 0.1 bar$_g$ (above) and 0.7 bar$_g$ (below).

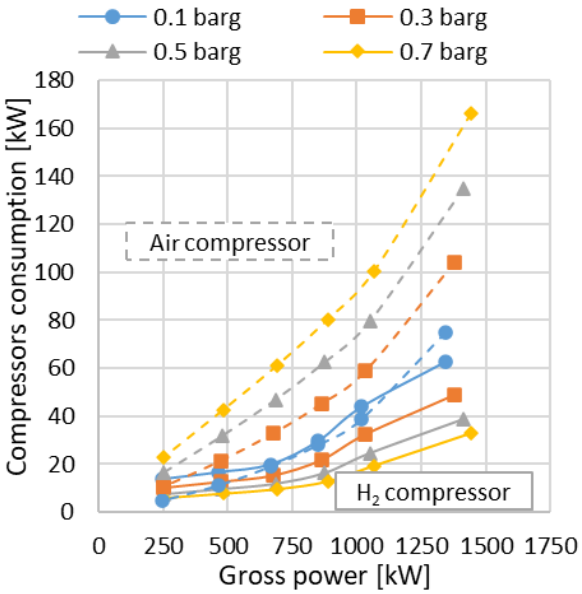

Figure 4.4 - Air and hydrogen compressors power consumptions Vs gross power, for current density ranging between 20% and 150% of the nominal value and for different levels of stack pressurization.

On the whole, when the backpressure is increased, the air compression consumption rises faster than the drop in hydrogen compression consumption. It is concluded that a pressure gain always leads to higher power consumption from the auxiliaries, independently on the current density.

The effect of increasing the backpressure on the net efficiency is obtained combining the positive effect on the stack generation and the negative effect on the compressors consumption.

This project has received funding from the Fuel Cells and Hydrogen 2 Joint Undertaking under grant agreement No 779430. This Joint Undertaking receives support from the European Union's Horizon 2020 research and innovation programme, Hydrogen Europe and Hydrogen Europe research.

Table 4.2 summarizes the values of net electric power generation and net electric efficiency, for increasing stack backpressure and significant values of current density (representing the minimum load, the nominal load, and an intermediate load value). Hydrogen consumption varies between 133 Nm^3/h at minimum current and 662 Nm^3/h at nominal current.

Table 4.2 - Plant performances for increasing backpressure, with and without expander, at full and partial load.

p [bar_g]	i [A/cm^2]	P_{gross} [kW_{el}]	η_{gross} [$\%_{LHV}$]	P_{net} [kW_{el}]	η_{net} [$\%_{LHV}$]
0.1	0.2	246.79	62.01	213.13	53.56
	0.6	666.06	56.16	590.73	49.81
	1	1016.89	51.51	878.93	44.53
0.3	0.2	249.13	62.60	213.56	53.66
	0.6	676.05	57.00	591.28	49.86
	1	1033.35	52.35	886.09	44.89
0.5	0.2	251.29	63.15	212.40	53.37
	0.6	684.41	57.71	588.70	49.64
	1	1049.80	53.18	888.92	45.03
0.7	0.2	253.58	63.72	210.46	52.89
	0.6	693.11	58.44	585.38	49.36
	1	1066.18	54.01	889.25	45.05

At low values of net power, the minimum net efficiency is obtained at the highest pressure (0.7 bar_g) while the maximum value is obtained at 0.3 bar_g. The situation changes for higher net power: above about 750 kW_{el} of net power generation, the highest net efficiency is obtained at 0.5 bar_g and the lowest at the minimum backpressure (0.1 bar_g). Finally, above about 880 kW_{el} net power, a further slightly increase in the net efficiency is obtained increasing the backpressure up to 0.7 bar_g. Therefore, the optimal operating strategy would consider operating at 0.3 bar_g at minimum load, increasing then the stack backpressure up to 0.7 bar_g while increasing the load. The maximum net electric efficiency that the plant is able to reach by adopting this operation strategy is ~45%$_{LHV}$ at nominal current and up to ~54%$_{LHV}$ when the current decreases to its minimum value.

4.1.2 Use of air expanders for energy recovery from cathode exhausts

This section aims at assessing the effectiveness of air expanders adoption, showing in which conditions this solution may bring significant advantages. For air compression, the same solution considered in the simulation of Section 4.1.2 is adopted. Two expanders are considered, adopting a volumetric technology similar to the compressor one. Each expender is coupled with a compressor on a single shaft. In this way, the expanders directly provide mechanical power to the compressors. Air cooling, water recovery and air release into the atmosphere are then performed as in the previous option. Other options for the coupling of the expander with the compression unit (e.g. electrical coupling) are also possible, but not considered here.

The resulting plant layout is shown in Figure 4.5.

This project has received funding from the Fuel Cells and Hydrogen 2 Joint Undertaking under grant agreement No 779430. This Joint Undertaking receives support from the European Union's Horizon 2020 research and innovation programme, Hydrogen Europe and Hydrogen Europe research.

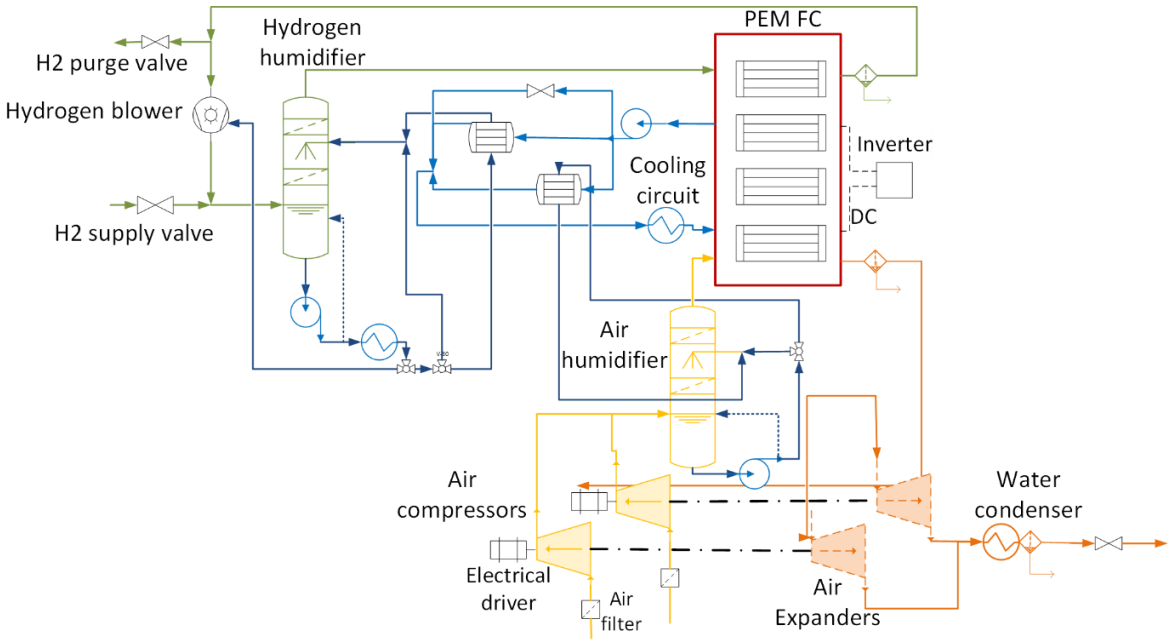

Figure 4.5 - MW-scale FC plant configuration including air expanders.

With respect to the case without the expanders, the auxiliaries consumptions are decreased by the expanders power generation, that is shown in Figure 4.6 as a function of the gross power. As for the air compressors consumption, the expanders generation increase by increasing the FC gross power (due to the increased air flow processed) and by increasing the FC stacks backpressure (due to the increased pressure change).

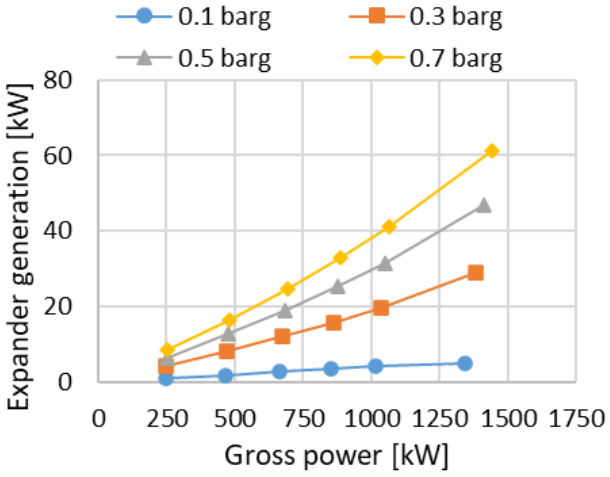

Figure 4.6 - Air expander power generation Vs FC gross power, for current density ranging between 20% and 150% of the nominal value and for different levels of stack pressurization.

The resulting total auxiliaries power consumption and the net efficiency of the plant are shown in Figure 4.7 as a function of the FC gross and net power respectively, in comparison to the values obtained without the expander.

This project has received funding from the Fuel Cells and Hydrogen 2 Joint Undertaking under grant agreement No 779430. This Joint Undertaking receives support from the European Union's Horizon 2020 research and innovation programme, Hydrogen Europe and Hydrogen Europe research.

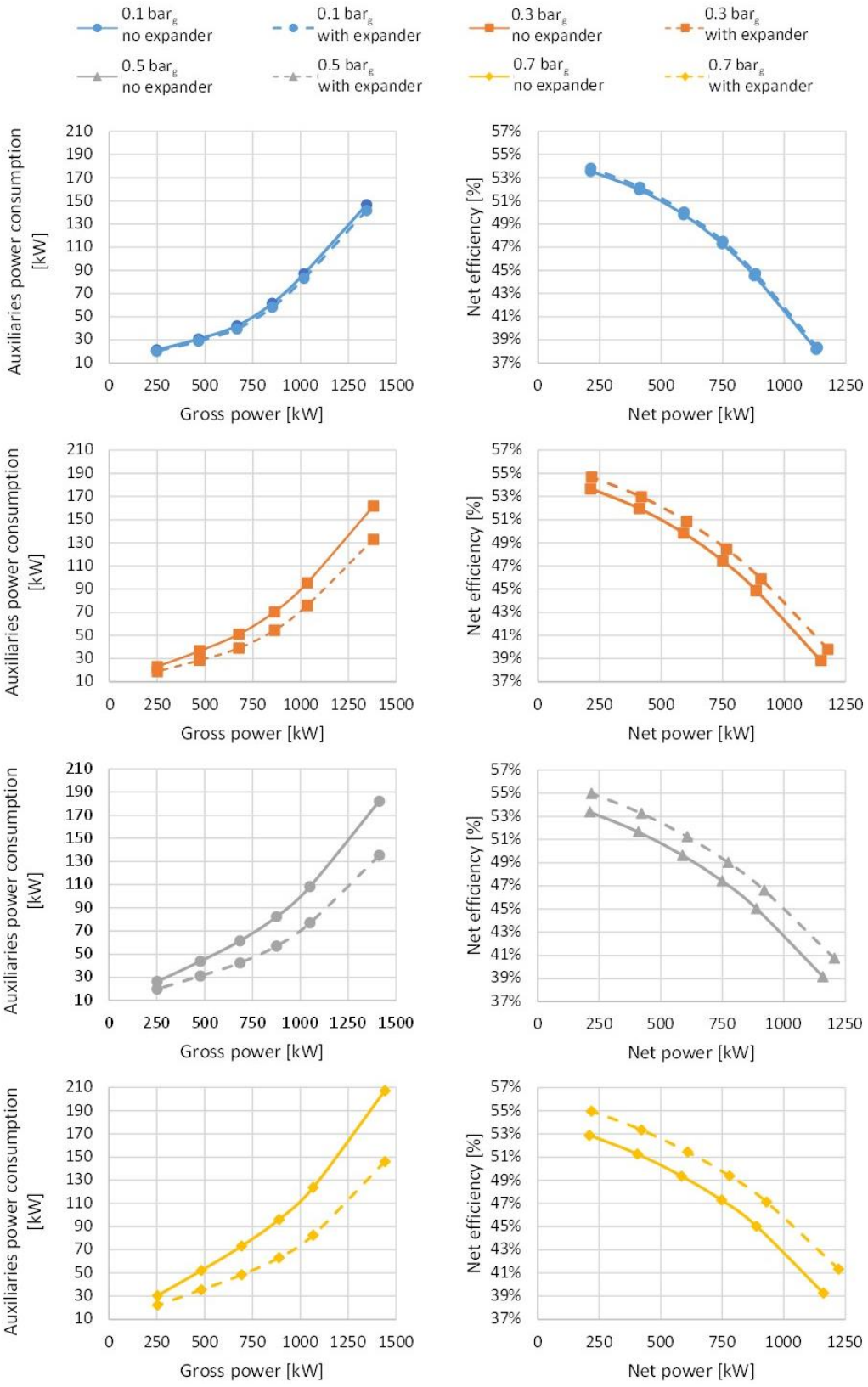

Figure 4.7 - Auxiliary consumption vs gross power (left side column) and net efficiency vs net power (right side column), for current densities ranging between 20% and 150% of the nominal value, for different levels of stack pressurization, with and without an air expander for energy recovery.

This project has received funding from the Fuel Cells and Hydrogen 2 Joint Undertaking under grant agreement No 779430. This Joint Undertaking receives support from the European Union's Horizon 2020 research and innovation programme, Hydrogen Europe and Hydrogen Europe research.

With the expander, an increase in pressure does not leads always to an increase in the total auxiliaries consumption. Simulations show that the pressure that minimizes the net auxiliary consumption is 0.3 bar_g and the one that maximizes it is 0.7 bar_g.

The expander allows reaching both higher net power and higher net efficiency, especially in pressurized conditions. Indeed, at 0.1 bar_g the net efficiency gain brought about by the installation of the air expander is not appreciable due to the very low expander pressure ratio. At higher backpressure, the expander becomes more effective. The net efficiency gain with the introduction of the air expander is equal to 1%$_{pt}$ at 0.3 bar_g, 1.6%$_{pt}$ at 0.5 bar_g and 2.1%$_{pt}$ at 0.7 bar_g. Furthermore, when operating with the maximum current, at 0.7 bar_g a gain in the maximum net power of nearly 61 kW is obtained. Finally, the highest net efficiency is obtained at 0.7 bar_g for net loads above 600 kW_{el}, while for lower loads a slight increase (+0.01% at minimum load) in the net efficiency is obtained by reducing the backpressure to 0.5 bar_g. Thus, the plant can be practically operated at constant backpressure (0.7 bar_g), simplifying the control of the system without impacting on the system efficiency. Net efficiency up to ~47% $_{LHV}$ and ~55% $_{LHV}$ are reached for current density equal to the nominal and the minimum values, respectively.

4.2 Warm up optimization

The dynamic model of the system allows simulating cold start-ups, to identify the time required by the system to reach the nominal point when started after a long shut-down period, when all the components and the cooling fluid are at ambient temperature. The warm-up time is indeed an important parameter to identify the flexibility of the system and is required to plan when to start-up the system, according to the services it has to provide.

Warm-up simulations are performed both with the 100 kW and with the 1 MW system models, and for two different warm-up procedures: i) a warm-up procedure decided by the Grasshopper consortium to limit stack degradation, limiting the current density at low coolant and air temperature, and ii) a warm-up procedure with no limits on the current at low temperature, and a maximum current rate of increase of 2.5%/s. Additionally, a sensitivity analysis is performed to identify which parameters mostly influence the warm-up duration and to identify strategies to speed up the warm-up process. The simulated cases are identified in Table 4.3, while Table 4.4 characterizes, for each case, the system in term of water inventory (i.e, the water content in the main plant components at the beginning of the simulation). This information is important to understand the simulation results, since the heat capacity of the water influences the overall thermal inertia of the system.

This project has received funding from the Fuel Cells and Hydrogen 2 Joint Undertaking under grant agreement No 779430. This Joint Undertaking receives support from the European Union's Horizon 2020 research and innovation programme, Hydrogen Europe and Hydrogen Europe research.

Table 4.3 – Characterization of warm-up simulated cases.

Plant size	Case	Warm-up procedure	Changes in plant layout / initial state
100 kW	**A**	Grasshopper	-
	B	Fast current increase	-
1 MW	**A**	Grasshopper	-
	B	Fast current increase	-
	C	Grasshopper	Pipes length 1/3 (compact system)
	D	Grasshopper	Halved water in humidifiers tanks

Table 4.4 – Water content (inventory) in the main plant component for the 100 kW and the 1 MW units and simulations cases A, B, C and D, defined in Table 4.3.

	100 kW	**1 MW system**		
	A-B	**A-B**	**C**	**D**
Coolant in pipes	84.8 L (26.1%$_{tot}$)	2416.5 (49.0%$_{tot}$)	711.9 L (23.2%$_{tot}$)	2416.5 L (64.0%$_{tot}$)
Water in air humidifiers pipes	4.7 L (1.5%$_{tot}$)	102.1 (2.1%$_{tot}$)	23.6 L (0.8%$_{tot}$)	102.1 L (2.7%$_{tot}$)
Water in H2 humidifiers pipes	3.3 L (1.0%$_{tot}$)	102.3 L (2.1%$_{tot}$)	16.3 L (0.5%$_{tot}$)	102.3 L (2.7%$_{tot}$)
Water in air humidifiers tanks	165 L (51.0%$_{tot}$)	1650 L (33.4%$_{tot}$)	1650 L (53.9%$_{tot}$)	825 L (21.9%$_{tot}$)
Water in H2 humidifiers tanks	66 L (20.4%$_{tot}$)	660 L (13.4%$_{tot}$)	660 L (21.6%$_{tot}$)	330 L (8.7%$_{tot}$)
Total	323 L	4930.9 L	3061.8 L	3775.9 L

Results of the simulations are reported in Table 4.5 in term of: time required for the system to reach full load and nominal operating conditions ('Warm-up time'), amount of hydrogen consumed during the warm-up time, net electric energy that is delivered during the warm-up time (assuming that no limit on the net power are imposed) and specific hydrogen consumption during the warm-up time.

Comparing Case A and Case B, regardless the plant size, the time required to reach the nominal setpoint is lower in Case B. In this case, the current reaches the nominal value in 1 minute and 40 seconds, while in Case A the current rise is proportional to the temperature and the nominal current is reached only at the end of the warm-up process (see Figure 4.8). The faster temperature rise in Case B is therefore determined by the higher thermal losses of the stack (higher power and lower efficiency) at a higher current. It can be concluded that the choice of the warm-up strategy strongly affect the warm-up time.

This project has received funding from the Fuel Cells and Hydrogen 2 Joint Undertaking under grant agreement No 779430. This Joint Undertaking receives support from the European Union's Horizon 2020 research and innovation programme, Hydrogen Europe and Hydrogen Europe research.

Table 4.5 - Warm-up simulations results: warm-up time, amount of hydrogen consumed, delivered electric energy generated and average specific hydrogen consumption during warm-up.

	100 kW		1 MW			
	A	**B**	**A**	**B**	**C**	**D**
Warm-up time	59 min	20 min	2 h 38 min	34 min	46 min	2 h 27 min
Consumed hydrogen during warm-up [kg_{H2}]	2.1	1.9	51.2	32.0	16.1	49.4
Delivered energy during warm-up [kWh_{el}]	25.3	22.4	608.7	372.5	192.4	588.3
Specific consumption during warm-up [kg_{H2}/kWh_{el}]	0.08	0.08	0.08	0.08	0.08	0.08

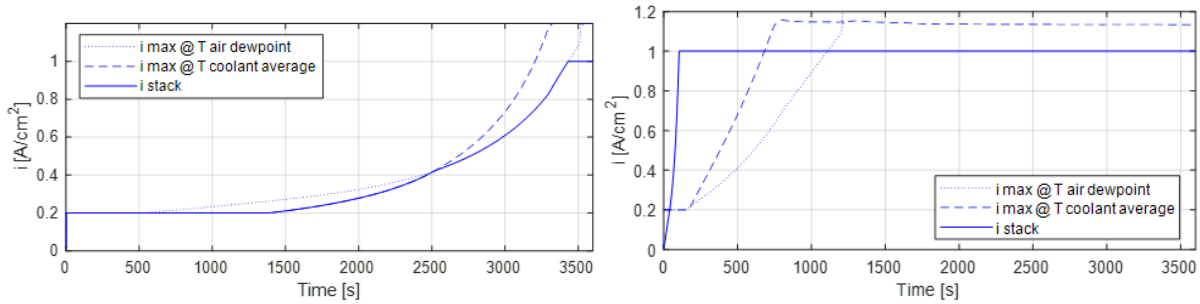

Figure 4.8 – Current increase over time for case A (left) and case B (right), for the 100 kW unit.

The impact of the plant size is assessed comparing the results of case A, for the 100 kW and the 1 MW units. The time required to reach the nominal current density (see Figure 4.9) as well as the time required to reach the nominal operating point are much higher for the 1 MW plant with respect to the 100 kW plant (+165%). The main reason is that, due to the longer and bigger pipes connecting the plant components, the amount of coolant and water that has to be heated increases consistently. Indeed, in scaling up the system, it has been assumed that the pipes connecting the system components in the 1 MW plant are 3 times longer than in the 100 kW plant. Additionally, the diameter of each pipe is computed in order to keep constant the total pressure drops, thus leading to a lower velocity in the pipes. This assumption affects the warm-up time for two reasons: more water and coolant fluid is present in the piping system (see Table 4.4, where the total amount of liquid is +53% with respect to 10 times the amount of liquid in the 100 kW system) increasing the overall system thermal inertia, and the time needed for the coolant fluid to go from the FC stack to the heat exchangers and back to the stack increases. Furthermore, while in the 100 kW system the coolant fluid in the pipes

This project has received funding from the Fuel Cells and Hydrogen 2 Joint Undertaking under grant agreement No 779430. This Joint Undertaking receives support from the European Union's Horizon 2020 research and innovation programme, Hydrogen Europe and Hydrogen Europe research.

represents about 26% of the total liquid volume, in the 1 MW system it represents 49%, explaining why in this case the limiting temperature is always the coolant temperature. Indeed, most of water in the MW system is in the coolant pipes, while in the 100 kW unit the majority was in the air humidifier tank.

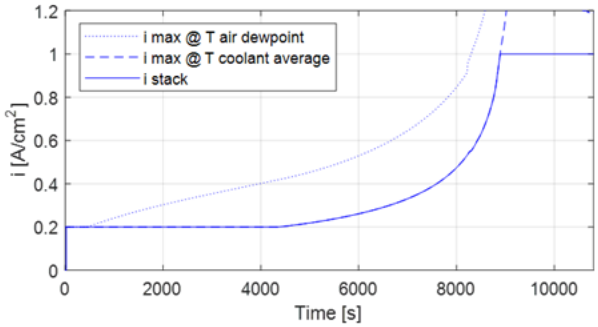

Figure 4.9 – Current increase over time for case A, for the 1 MW unit.

Finally, the sensitivity analysis allow assessing the effectiveness of two methods proposed to reduce the warm-up time in the MW-size plant.

The design of a compact system is very effective. In case C, assuming that the pipes connecting the system components have the same length as in the 100 kW plant and the pipes diameters leads to the same overall pressure drops as in the 100 kW plant, a 71% reduction in the warm-up time is obtained (corresponding to -23% with respect to the 100 kW case). In this case, the total amount of liquid in the system (see Table 4.4) is -5% with respect to 10 times the amount of liquid in the 100 kW system and -38% with respect to the base case for the 1 MW system. As regard the amount of coolant in the pipes, it is -16% with respect to 10 times the amount of coolant in the 100 kW system.

The reduction of the amount of water in the humidifier tanks is less effective. In CASE D, the thermal inertia of the system is decreased through the halving of the water content in the humidifiers tanks, shows only a 9% reduction of the warm up time. In this case, the total amount of liquid in the system (see Table 4.4) is +17% with respect to 10 times the amount of liquid in the 100 kW system, and -5% with respect to the amount of liquid in the base 1 MW case.

This project has received funding from the Fuel Cells and Hydrogen 2 Joint Undertaking under grant agreement No 779430. This Joint Undertaking receives support from the European Union's Horizon 2020 research and innovation programme, Hydrogen Europe and Hydrogen Europe research.

5 Economic considerations on plant scale-up

The main economic objective for GRASSHOPPER project, with regards to the next-generation MW-size Fuel Cell Power Plant unit (FCPP), is to achieve an estimated CAPEX below 1,500 EUR/kW_e at a yearly production rate of 25 MWe.

The predominant economic items have been evaluated during the design of the MW size FCPP. As it can be observed in the following Figure, fuel cell stacks represent the 39% of the total CAPEX, followed by the mechanical BoP costs.

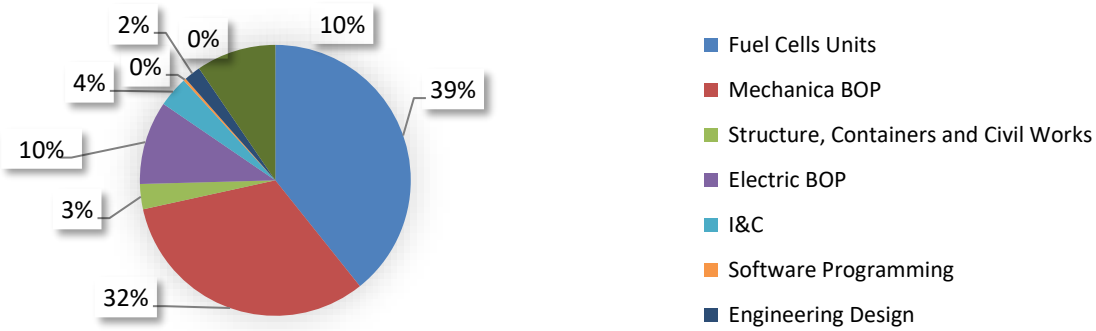

Figure 5.1 – Capex distribution identified for MW-scale plant

The evaluation of potential improvements in MW scale FCPP offer the possibility to give some recommendations related to costs:

- Further reduction in the costs of FC will have the largest impact on the overall CAPEX of the plant. Since the mechanical BOP is composed of many small equipment, the margin of cost reduction in the short-mid term on them is quite low.
- The recent increase in steel and other material costs will significantly affect the mechanical BOP weight on the overall CAPEX. By further optimizing the different materials used in the plant, some of this impact could be reduced.
- The use of standard shipment container is ideal for plug and play solutions and transport. However, investing more money in the adaptation of said container will result in more savings during construction and maintenance.
- With the standardization and large-scale manufacturing, additional cost could be reduced in the construction and commissioning of the plant.

This project has received funding from the Fuel Cells and Hydrogen 2 Joint Undertaking under grant agreement No 779430. This Joint Undertaking receives support from the European Union's Horizon 2020 research and innovation programme, Hydrogen Europe and Hydrogen Europe research.

6 Conclusions

This work has proposed effective solutions to improve the layout and the operative strategy of a 1 MW PEM FC power plant, to scale-up the 100 kW Grasshopper pilot plant for commercialization.

Stationary simulations allowed comparing the plant net efficiency, both at nominal and at partial load, for different plant layouts and operating conditions. The simulations considered the possibility of pressurizing the system and also recovering energy from the stack cathode exhausts, adapting features of automotive systems to the stationary unit. Results show that increasing the pressure always allows to increase the FC stack gross efficiency, while the net efficiency depends also on how the auxiliaries consumption (mainly the compressors consumption, representing at least 87% of the total auxiliaries consumption) changes. The hydrogen compressor, with a limited control of the flow rate, consumes less at higher pressures and lower current density, where the pressure losses are minimized. The air compressor consumption and the air expander generation increase with increasing current density and backpressure, due to the increased flow rate and pressure change. Comparing the cases with and without the expanders, higher net efficiencies are reached with the expanders, especially in pressurized conditions. This allows reaching higher net power outputs, fixed the current density (i.e., the hydrogen consumption). Furthermore, while without the expander the optimal operation strategy requires to change the stack backpressure while changing the load, with the expander it is possible to operate at constant pressure without a negative impact on the net efficiency. The use of two compressors in parallel configuration and the installation of the expander are therefore recommended on the efficiency point of view.

Dynamic simulations allowed studying the system warm-up, pointing out the strong impact of the adopted warm-up strategy on the warm-up time. Simulations results showed that the system temperature increases much faster when higher current density are considered. Additionally, the simulations pointed out the main criticalities of the scale-up. An increase in the plant size have shown to increase the warm-up time. To limit this effect it is important to limit the amount of water in the plant, e.g. limiting the water in the humidifiers tanks or using short pipes to connect the components. The main recommendation for the construction of a flexible power plant is to design a compact system.

On the economic point of view, improvements could be done for the design of the MW- size FCPP by optimizing the FC costs and the use of different materials, by evaluating the optimal FC container and by adapting the manufacturing methods. The economic items of CAPEX have been analyzed for the MW- size FCPP.

This project has received funding from the Fuel Cells and Hydrogen 2 Joint Undertaking under grant agreement No 779430. This Joint Undertaking receives support from the European Union's Horizon 2020 research and innovation programme, Hydrogen Europe and Hydrogen Europe research.

7 References

[1] S. Campanari, G. Guandalini, J. Coolegem, J. Ten Have, P. Hayes, and A. H. Pichel, "Modeling, Development, and Testing of a 2 MW Polymeric Electrolyte Membrane Fuel Cell Plant Fueled with Hydrogen from a Chlor-Alkali Industry," *J. Electrochem. Energy Convers. Storage*, vol. 16, no. 4, pp. 1–9, 2019, doi: 10.1115/1.4042923.

[2] A. J. L. Verhage, J. F. Coolegem, M. J. J. Mulder, M. H. Yildirim, and F. A. De Bruijn, "30,000 h operation of a 70 kW stationary PEM fuel cell system using hydrogen from a chlorine factory," *Int. J. Hydrogen Energy*, vol. 38, no. 11, pp. 4714–4724, 2013, doi: 10.1016/j.ijhydene.2013.01.152.

[3] "EU project Grasshopper." http://www.grasshopperproject.eu/ (accessed Jun. 06, 2020).

[4] "AspenTech software website." https://home.aspentech.com/ (accessed Jun. 06, 2020).

[5] E. Crespi, G. Guandalini, S. Gößling, and S. Campanari, "Modelling and optimization of a flexible hydrogen- fueled pressurized PEMFC power plant for grid balancing purposes," vol. 6, 2021, doi: 10.1016/j.ijhydene.2021.01.085.

[6] "AERZEN webpage." https://www.aerzen.com/it/prodotto/soffiatori-delta-blower-generation-5/performance.html.

This project has received funding from the Fuel Cells and Hydrogen 2 Joint Undertaking under grant agreement No 779430. This Joint Undertaking receives support from the European Union's Horizon 2020 research and innovation programme, Hydrogen Europe and Hydrogen Europe research.